JOURNAL OF MATERIALS SCIENCE 14 (1979) 2459–2470

Electron metallography of the aluminium–water vapour reaction and its relevance to stress-corrosion susceptibility

G. M. SCAMANS, A. S. REHAL
Alcan Laboratories Limited, Banbury, Oxon., UK

The reaction of filmed surfaces of aluminium and certain aluminium alloys with water vapour saturated air at 70° C has been morphologically studied at high resolution using a JEOL 100C Temscan. Electron-transparent specimens, reacted for up to 24 h, have been examined using a combination of SE (secondary electron) and STE (scanning transmission electron) imaging modes to examine both the surface attack detail and the underlying microstructure of precisely located areas. Reaction on filmed surfaces is initiated by a hydrogen-induced blistering of the amorphous oxide film, the fracture of which results in the development of pseudoboehmite and bayerite on the bared metal surface. Alloying additions of magnesium localize the breakdown reaction at grain boundary–surface intersections, although this effect can be controlled by raising the solution heat treatment temperature to 550° C. The localization of the reaction results in hydrogen penetration of grain boundaries in magnesium-containing alloys, and this promotes a loss of grain-boundary strength and may lead to alloy failure by stress-corrosion cracking.

1. Introduction

Certain important groups of aluminium alloys, notably the 7000 series AlZnMg alloys, become hydrogen-embrittled on exposure to water vapour and this phenomenon, which is described as stress-corrosion cracking when observed under the conjoint action of stress and environment, severely limits their usage [1, 2]. Thus an understanding of the reaction with water vapour is of considerable importance, particularly as highly susceptible alloys may fail in environments as apparently innocuous as ambient air. In order to understand the reaction on the ternary AlZnMg alloy, it is first necessary to study the behaviour of pure aluminium and then to observe how this is modified by additions of zinc and magnesium, both singly and in combination. Additionally, in order to stimulate the reaction, both increases in temperature and humidity are appropriate as such changes, i.e. to 70° C and 100% r.h., have been shown to cause acceleration of cracking without changing the embrittlement phenomenon [1].

Background information for this study was first obtained from a study of the literature on the aluminium–water reaction at 70° C, concentrating on work reported where pre-filmed surfaces were the starting condition rather than "clean" surfaces.

1.1. The reaction of aluminium with water

The reaction of aluminium with water in the liquid phase has received significant attention for over fifty years and the results of this considerable amount of work have recently been comprehensively reviewed [3]. Basically, the reaction of aluminium with water at 70° C produces a duplex film consisting of a layer of pseudoboehmite next to the metal and a layer of bayerite crystals in contact with the solution [3, 4]. Pseudoboehmite is an aluminium oxyhydroxide similar to boehmite (AlOOH) but containing more water, whereas

0022–2461/79/102459–12 $03.20/0

bayerite is a form of aluminium hydroxide ($Al(OH)_3$). However, pseudoboehmite and bayerite are thermodynamically metastable phases at 70° C and 1 atm. pressure, the equilibrium phase being gibbsite. Significantly, the formation of either 1 mole or pseudoboehmite or bayerite involves the production of 1.5 moles of hydrogen.

The reaction on filmed surfaces involves an induction period at 70° C of the order of a minute; this is followed by a period of rapid growth, which is then superceded by much slower growth after ten minutes. During the induction period the amorphous oxide film thickens to about 100 Å [4] and is penetrated by either protons, hydroxyl ions and/or water until conditions for hydrolysis are established and a soluble aluminium species is produced. Dissolution is then accompanied by the simultaneous precipitation of hydrous oxide which subsequently transforms to pseudoboehmite. When a layer of pseudoboehmite has formed, the rapid growth rate period ends and further growth must occur by diffusion through this layer, the need for dissolution to occur as a stage in the reaction being inferred from studies involving the ageing of hydroxide gels which similarly produce pseudobeohmite [5]. The rate-determining step during the slow growth stage is probably the inward diffusion of water rather than the outward migration of Al^{3+} ions which suggests that new hydrous oxide develops under the existing film [6]. The mode of bayerite formation is not clear but this is also considered to involve a dissolution and precipitation process, presumably of the pseudoboehmite surface in contact with the solution. Measured film thicknesses are of the order of 2 to 3 μm and growth ceases where the surface is covered by bayerite [7].

The bayerite crystals are not embedded in the surface nor joined to the pseudoboehmite and may be removed by mechanical means or with adhesive tape. They appear as cones, wedges, rods and hourglass figures and these diverse shapes have been given the general classification of somatoids [3]. Pseudoboehmite takes the form of platelets which appear as fibrils or needles when viewed by transmission electron microscopy. Bayerite and pseudoboehmite are therefore readily identifiable by their characteristic morphologies.

The reaction of aluminium with water vapour as opposed to water at 70° C has received little attention. Vedder and Vermilyea [8] concluded from their vapour-phase studies at 90 to 100° C that condensation was essential for hydroxide growth to occur and that additionally the induction period was greatly extended and the growth rate was much reduced; for example the induction period increased to 27 h, and after 70 h reaction the weight gain was only equivalent to that achieved within 25 min in liquid water. No morphological information was reported in this work although it was suggested that the same dissolution/precipitation processes which form pseudoboehmite and bayerite were in operation.

2. Experimental

2.1. Techniques

The electron microscope employed (the JEOL Temscan 100C) offers a unique advantage for the study of surface reactions in that both surface features and underlying microstructure of precisely located areas may be imaged sequentially. Thus the initial reaction sites could be examined in detail together with the underlying microstructure using SE (secondary electron) and STE (scanning transmission electron) imaging respectively. This mode of microscope operation has been termed combined SE/STE imaging. Significantly, the resolution in the SE mode at 100 kV accelerating potential is about 50 Å, which means that high quality scanning electron micrographs may be obtained at magnifications comparable to those normally used in transmission microscopy (TEI transmission electron imaging).

Oxide and hydroxide film thicknesses were also monitored by ellipsometry performed on bulk specimens given similar surface preparative treatments to the electron-transparent specimens [9]. These specimens were examined in a conventional scanning electron microscope at 30 kV.

2.2. Materials and specimen preparation

The compositional analysis of the d.c. cast ingots used in this study are shown in Table I. The starting material was cold-rolled sheet of the listed alloys (0.5 mm), together with superpurity aluminium (99.99%), This material was either annealed (Al 15 min at 310° C) or solution heat treated

TABLE I Compositional analyses of alloys (p.p.m.)

Cast no.	Fe	Mg	Si	Ti	Zn	B
A	<0.01	1.5	<0.01	0.010	4.30	12
B	0.11	<0.001	0.05	0.01	5.1	14
C	0.11	5.11	0.055	0.01	0.001	8

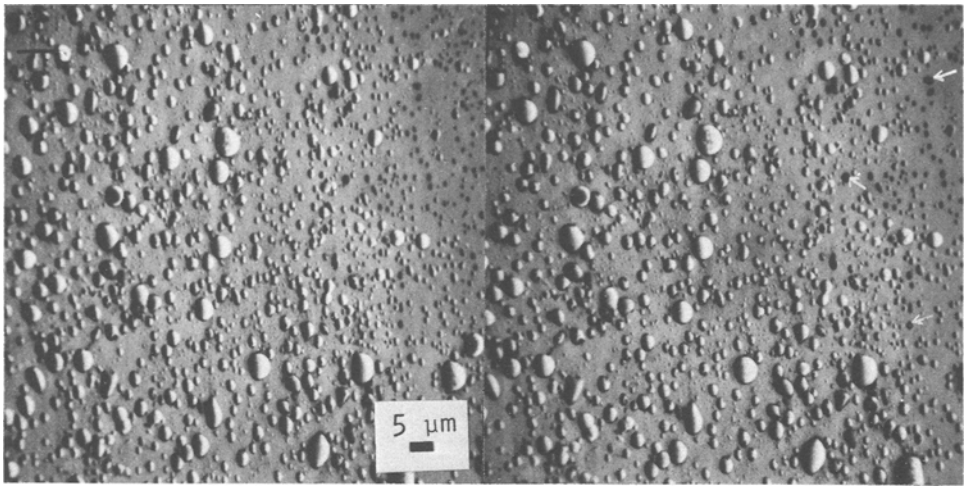

Figure 1 Stero pair of micrographs of surface film blisters on a bulk specimen of superpurity aluminium after reaction with WVSA at 70° C. Note the hemispherical nature of the blisters and the dark circular islands of reaction after blister fracture (arrowed).

(AlMg, AlZn 30 min at 450° C, AlZnMg 30 min at 465° C) and cold-water quenched. The AlMg alloy was also solution treated for 30 min at 350 and 550° C prior to cold-water quenching.

In order to prepare electron-transparent specimens, 3 mm discs were punched from the sheets and ground mechanically to 0.2 mm. Disc specimens were then prepared in the usual manner but employing fresh polishing solution made from Analar reagents and using a rigorous rinsing schedule in successive baths of methanol. The prepared specimens were monitored by light microscopy to ensure that no surface artifacts, i.e. dust particles, polishing solution residue, etc., were present after the rinsing treatment. After preparation, specimens were stored in a desiccator at room temperature for a minium period of 24 h in order for the normal amorphous γ-Al_2O_3 air-formed film to develop.

2.3. Specimen exposure and examination

Exposure to water vapour saturated air (WVSA) at 70° C was achieved by placing the specimens horizontally on a perspex holder in a humidity chamber at 100% r.h., under conditions where condensation of water vapour on the specimen

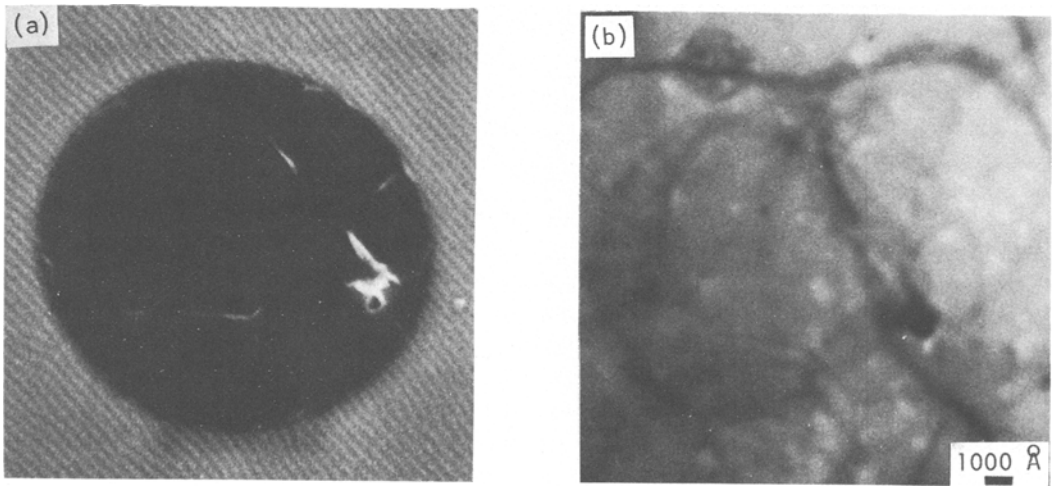

Figure 2 Detailed examination of a single reaction site in both (a) SE and (b) STE imaging modes. On superpurity aluminium there is no preferential siting of the defilming process.

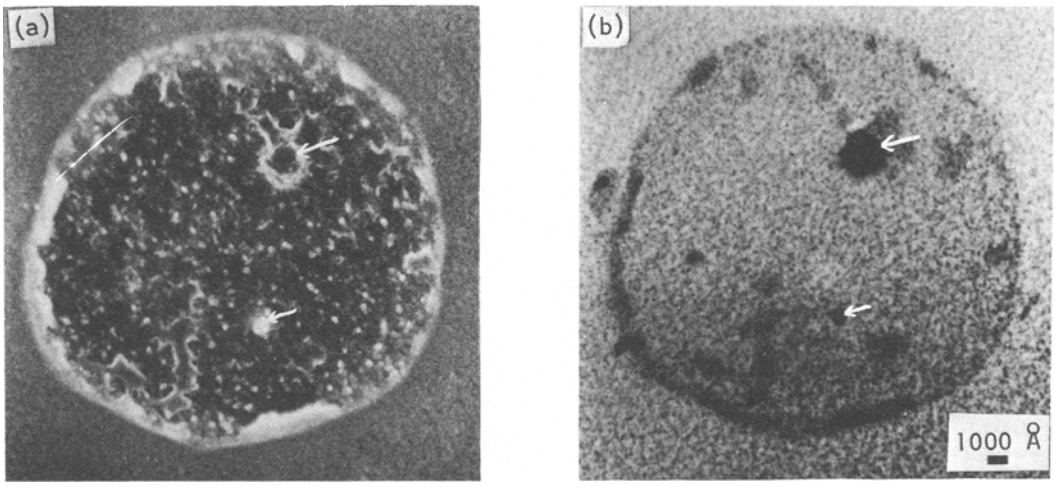

Figure 3 Combined (a) SEI and (b) STEI images of a reaction site on an aged AlZnMg alloy after 5 min reaction at 70° C. Note both the small crystallites and the larger crystals in (a) and that the larger crystals only are visible in (b) (as arrowed).

surface was observed. After exposure the specimens were examined immediately in the electron microscope using a liquid nitrogen cold trap at the specimen area to minimize surface contamination. Specimens were first examined using secondary electrons (SEI) and then transmitted electrons (STEI and TEI) in order that the surface microstructure could be imaged before surface artifacts due to contamination were produced. Subsequent imaging in transmission was not sensitive to this contamination. The SEI mode also enabled the reaction on electron-transparent regions to be compared with that on thicker areas.

The bulk specimens for ellipsometry and conventional SE imaging were given similar surface preparative treatments and were exposed to WVSA for up to six days at 70° C.

3. Results

3.1. Initiation

The earliest stages of hydroxide nucleation at 70° C were studied on specimens of superpurity aluminium. Exposure to WVSA at 70° C resulted in the random nucleation of circular "islands" of hydroxide within the first minute of reaction. Increased exposure times produced both further nuclei and lateral expansion and coalescence of existing islands until the specimen surface was covered in a hydroxide layer. The initial hydroxide growth was therefore rapid, but became progressively slower as less and less surface area was available for "island" nucleation. The reaction rate then depended on the rate of thickening of the hydroxide "islands". The reasons for the "island" growth morphology were initially not obvious and it was first thought that an "island" developed where a droplet condensed on the surface. However, close examination of reaction sites showed them to be regions where the surface had been effectively defilmed by a blistering mechanism. Blister visibility was greatly enhanced by thickening the amorphous surface film by storage in dry air after electro-polishing. This storage treatment did not affect the reaction kinetics. Regions where droplet formation did occur rapidly produced a much thicker hydroxide layer which extended over the area of droplet surface coverage. Conditions here were more typical of total immersion in water and such areas were regarded as artifactual in the context of the present study. No blisters or reaction sites were observed in the absence of condensation.

Initiation of reaction by surface film blistering is shown in the stereo pair of scanning electron micrographs in Fig. 1. This bulk specimen was held in dry air for 30 days after electro-polishing prior to reaction with water vapour at 70° C. On this specimen the majority of blisters in the surface oxide are unbroken and appear as hemispherical domes when viewed in stereo. Where blisters have burst a dark circular "island" of reaction can be seen on the surface (as arrowed). Fig. 2 shows a similar reaction site on a thin foil specimen which was exposed to WVSA for 5 min at 70° C after

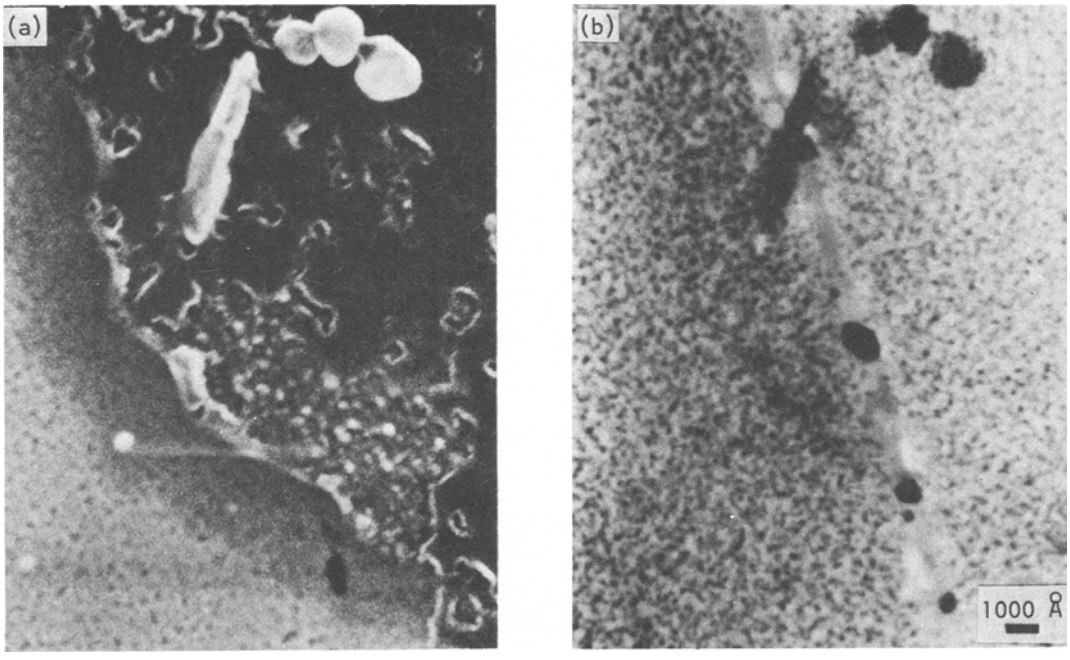

Figure 4 Close-up of a reaction site on an aged AlZnMg alloy. Note the underlying grain boundary in the STEI image (b) and the dark contrast at the blister periphery in the SEI image (a).

holding for 48 h at ambient temperature following electro-polishing. The secondary electron image (Fig. 2a) shows clearly the fractured surface film at the circumference of the reaction site, and surface film debris that has also collapsed onto the "island". The dark contrast is due to the low secondary electron emissivity of the thin hydrous oxide layer formed on the bared metal surface. The parallel lines are due to an electro-polishing artifact which is a feature of the underlying metal as the lines continue through the defilmed region. The scanning transmission image (Fig. 2b) barely discerns the reaction site, showing it to be a wholly surface feature, and this examination of the underlying microstructure could reveal no obvious metallurgical feature which had enhanced attack nucleation.

During exposure in dry air at room temperature after electro-polishing the surface film was observed to thicken from a value of less than 20 Å immediately after electro-polishing to approximately 50 Å after 48 h and to 150 Å after 30 days. Surface film thicknesses were determined by direct measurement on fractured blister walls and ellipsometric measurements on bulk specimens [9]. A standard treatment of 14 days at ambient temperature and 0% r.h. was instigated for subsequent experiments. This treatment gave a film thickness of less than 100 Å.

3.2. Alloying effects on blistering and hydroxide nucleation

Reaction of the alloy specimens in WVSA at 70° C also resulted in surface film blistering and defilming and similar reaction kinetics were determined. A typical reaction site on a thin foil specimen of the ternary AlZnMg alloy is shown in Fig. 3. In this case the alloy was artificially aged before thin foil preparation and was reacted for 5 min at 70° C. The surface film blister has again burst and rapid hydroxide growth has occurred on the defilmed area although the hydroxide layer is clearly duplex in nature (cf. Fig. 2). The larger hydroxide crystals, i.e. those visible under both SE and STE imaging modes (these are arrowed on the micrograph) produced single crystal electron diffraction patterns which were consistent with bayerite, although a full identification was not achieved. The STE image reveals the zinc and magnesium-rich precipitates in the underlying alloy and the thicker surface film renders the reaction site more clearly visible as compared to Fig. 2b.

A second example of the reaction on the ternary alloy, again in the aged condition, is shown at higher magnification in Fig. 4 after 5 min exposure. The SE image reveals the small crystallites which are about 200 Å in diameter, the dark structureless regions of blister wall debris and the larger hydroxide crystals, which are probably

bayerite. Again, only these large (about 1500 Å) crystals are observed in the STE image. The STE image does however show an underlying grain boundary. At the circumference of the reaction site in the SE image the surface film shows dark contrast over a region approximately 2000 Å wide. This feature, which was frequently noted, was attributed to decohesion of the amorphous oxide–metal interface by hydrogen generated on the reaction site.

Preferential reaction at grain boundary–surface intersections was a characteristic of the reaction on both the magnesium-containing alloys whereas the aluminium–zinc binary alloy behaved similarly to pure aluminium. This grain-boundary attack selectivity was found to be a strong function of solution heat treatment temperature. The reaction on the Al–Mg binary alloy after solution heat treatment at 350 and 550° C is shown in Fig. 5. At 550° C random attack nucleation has occurred, whereas at 350° C there is a very strong selectivity of the attack at grain boundary–surface intersections, although it is of interest to note that not all the grain boundaries are attacked (see arrows). Some of the non-attacked boundaries were of low angle, and although unreacted high-angle boundaries were frequently discerned, an identification of the boundary type which provided this immunity was not achieved at this time. In both cases the specimens were reacted for

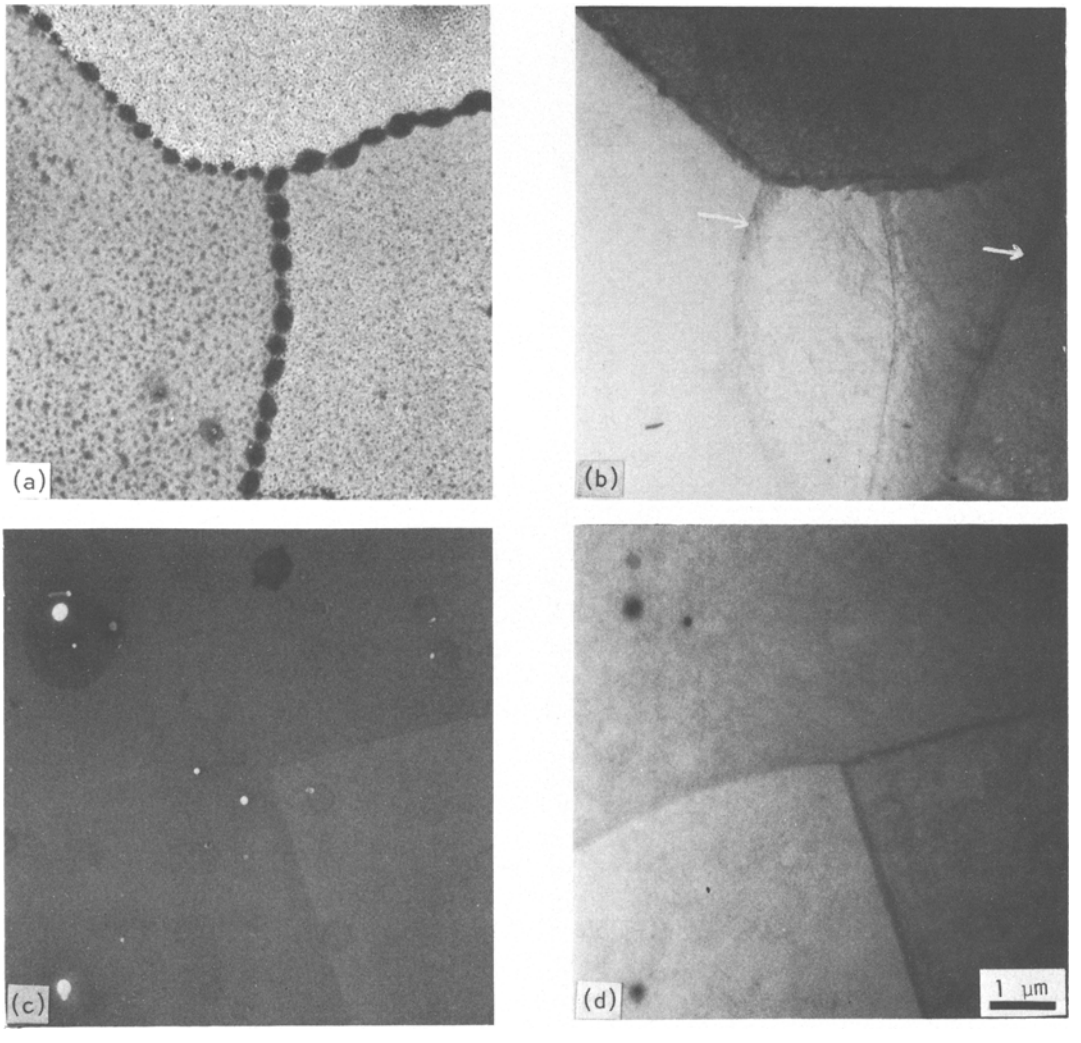

Figure 5 Effect of the temperature of solution heat treatment on the localization of reaction at grain boundary–surface intersections on the AlMg alloy after 10 min reaction at 70° C. At 350° C the attack is localized, although not all the grain boundaries are reacted, as shown in (a) and (b). At 550° C there is no preferential reaction siting and a general decrease in reactivity, as shown in (c) and (d).

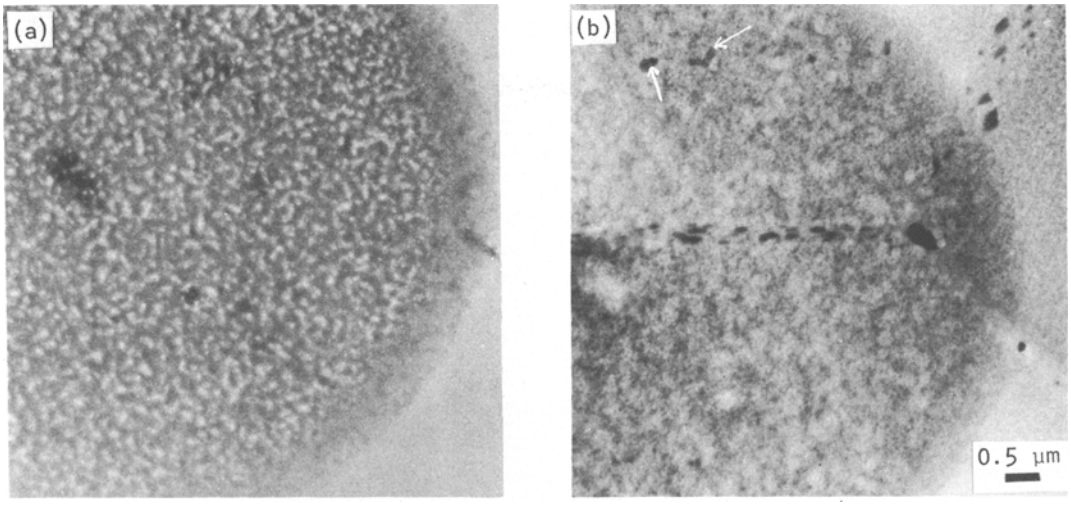

Figure 6 Development of the reaction site after 30 min at 70° C on the aged AlZnMg alloy. Note the development of pseudoboehmite from the small crystallites in (a) and the underlying grain boundary junction and the small bayerite crystals arrowed in (b).

10 min at 70° C. Heat treatment at 350° C also produced a general increase in surface reactivity as compared to treatment at 550° C. The intense reaction at grain boundaries was also observed after solution heat treatment at 450° C. It was attempted to measure magnesium segregation to grain boundaries as a function of solution heat treatment temperature using X-ray microanalysis; however, no significant increase in magnesium at the grain boundary could be detected. The white circular marks on Fig. 5c are due to surface contamination during microanalysis.

3.3. Hydroxide growth

A later stage of the reaction on the aged AlZnMg alloy is illustrated in Fig. 6, which shows a specimen after 30 min at 70° C. At this stage the hydroxide layer is sufficiently thick to become visible under STE imaging conditions. Again reaction has occurred preferentially at a grain boundary–surface intersection, and there is evidence of a decohered region at the "island" extremity. At this stage the reaction site is completely covered in a pseudoboehmite layer which appears to have developed from the small crystallites as shown in Figs. 3 and 4. The "bayerite" crystals are obscured on this reaction site but may just be discerned in the STE image (see arrows). This was not typical and such crystals could be observed, in the SE mode, on most reaction sites.

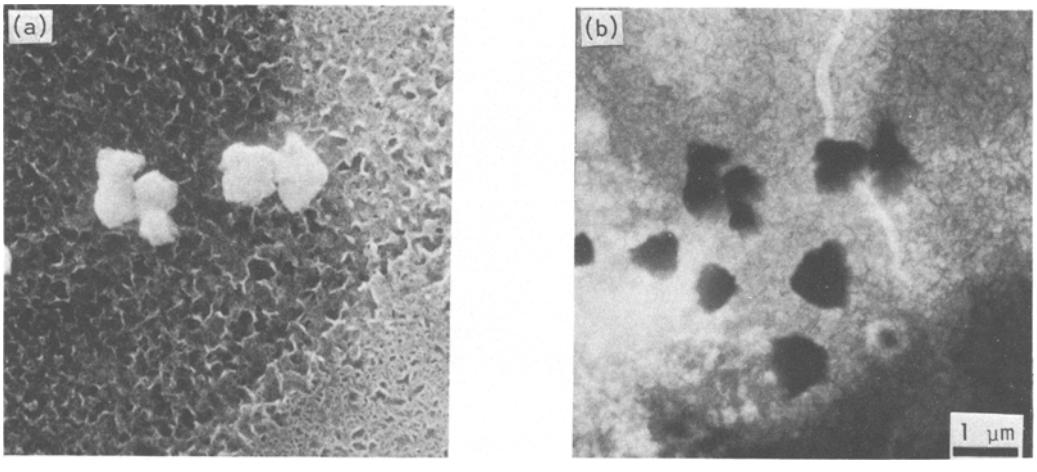

Figure 7 Thick duplex hydroxide layer after 24 h reaction at 70° C. Note that the bayerite crystals are on both surfaces of the foil. Both the bayerite and pseudoboehmite exhibit their characteristic morphologies.

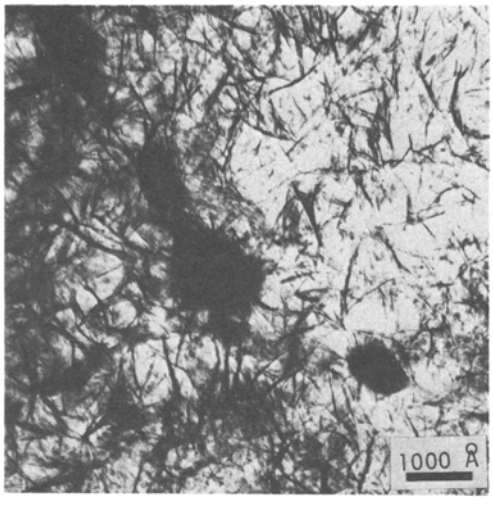

Figure 8 Transmission electron (TEI) image of the grain boundary penetration of bayerite after 24 h reaction of the aged AlZnMg alloy at 70° C.

After extended reaction times the hydroxide has the morphology shown in Fig. 7 which shows a specimen after 24 h reaction. The pseudoboehmite now exhibits its characteristic platelet morphology which appears as fibrils or needles in the STE image. Bayerite crystals or somatoids are obviously on both surfaces of the foil and there was some tendency for grain boundary penetration to occur as is shown in Fig. 8 using conventional TE imaging.

Hydroxide penetration into grain boundaries was only observed on specimens of the magnesium-containing alloys. However, for all the alloys studied, the crystalline hydroxide which develops into the characteristic bayerite somatoids was observed to nucleate and grow from the metal–oxide interface and not from the pseudoboehmite layer. This conflicts with reported observations made on hydroxide films grown under conditions of total immersion at 70° C

These conclusions were substantiated by ion-etching of thick hydroxide films grown on bulk specimens as shown in Fig. 9. The stereo pair of micrographs shows the pillars of bayerite extending from the metal surface. The pseudoboehmite has been preferentially etched away under the action of the ion beam and shadows of the bayerite somatoids are seen on the eroded surface. Cracks have developed in the thin remaining pseudoboehmite layer under the action of the ion beam. The small crystallites from which the pseudoboehmite platelets develop are apparent in this layer.

3.4. Effect of grain boundary attack localization

The effect of the localization of attack at grain boundary–surface intersections on the underlying microstructure was studied more conveniently using conventional TE imaging as, although the reaction sites themselves cannot be

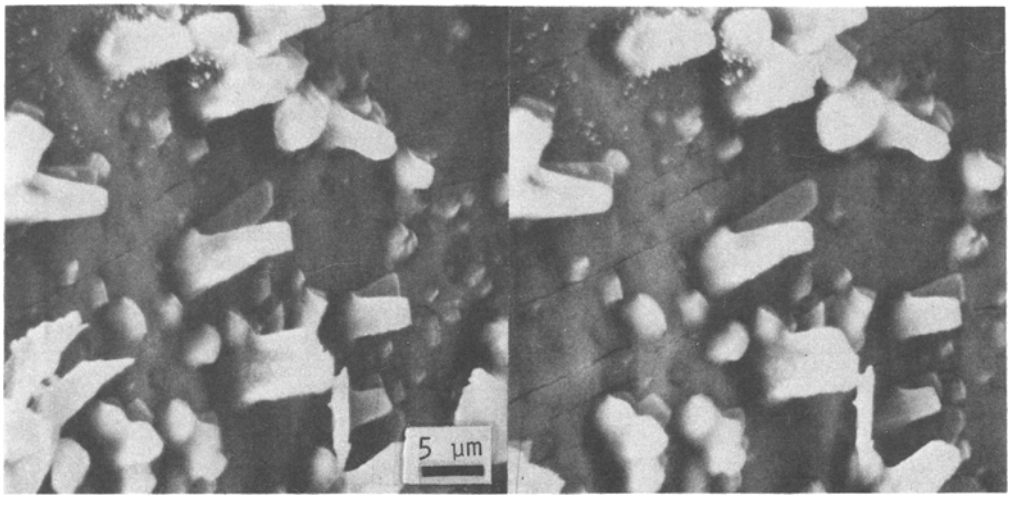

Figure 9 Stereo pair of micrographs of an ion-etched hydroxide film on an aged AlZnMg alloy after 6 days reaction at 70° C. Note that the bayerite crystals have grown from the metal–oxide interface.

discerned, evidence for hydrogen penetration of grain boundaries is readily apparent, as shown in Fig. 10 for an AlMg alloy specimen reacted for 10 min at 70° C. Fig. 10a, with the foil highly tilted and the grain boundary at high angle to the electron beam, shows hydrogen bubbles imaged by strain field contrast fully contained within the thin foil. Figs. 10b and c show the same grain boundary at a lower tilt angle under conditions of progressively weaker diffraction excitation. Significantly, in Fig. 10c bubbles can be seen on matrix dislocations where pipe diffusion of hydrogen away from the grain boundary has occurred. A detailed examination of hydrogen bubbles in AlZnMg reacted with WVSA at 70° C has already been published [10].

With increased exposure times the reaction sites could be imaged as shown in Fig. 11 where again a

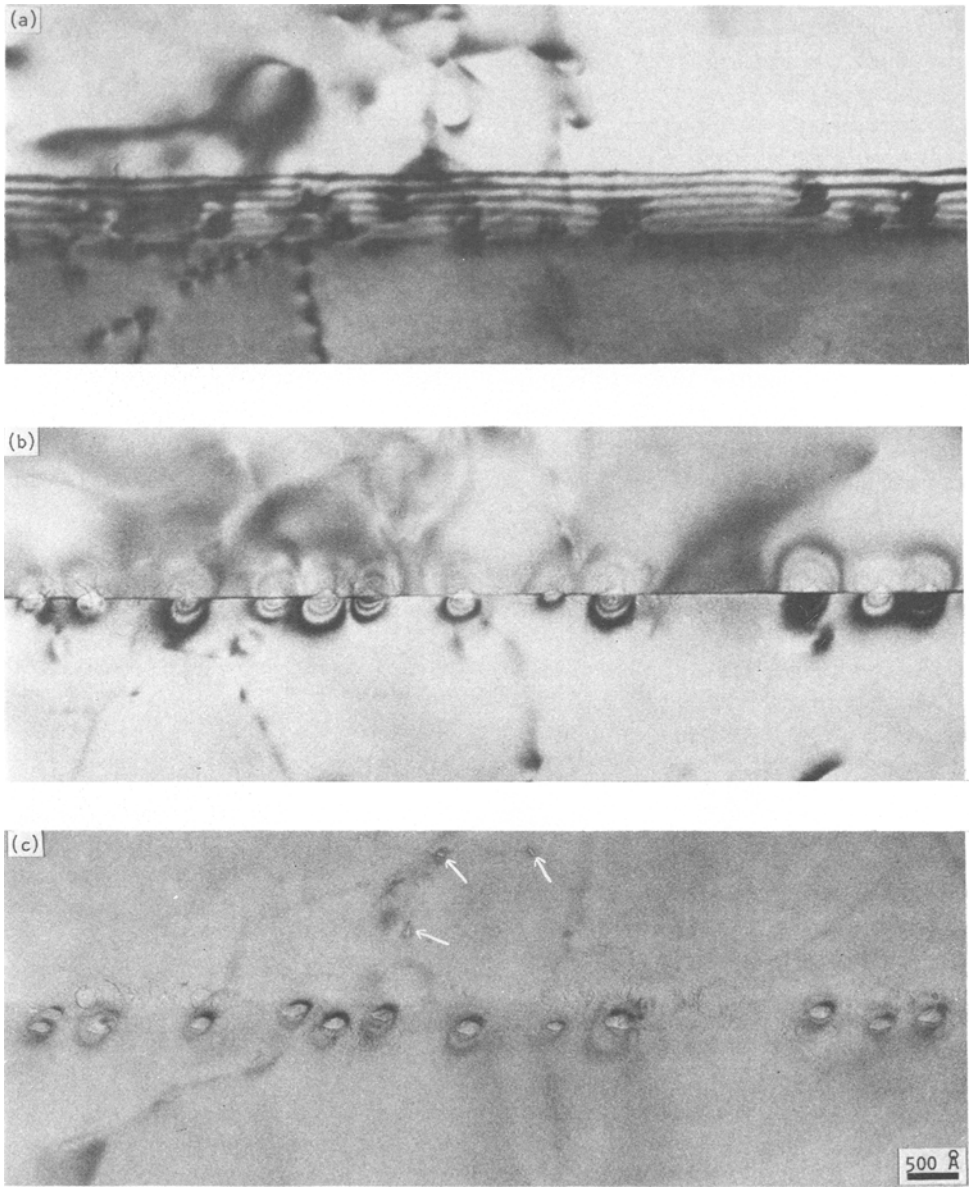

Figure 10 Bubbles of molecular hydrogen on grain boundaries of an AlMg alloy after 10 min reaction at 70° C. Note the bubbles on dislocations in (c) (arrowed).

high density of bubbles had developed on the grain boundary. Such reaction sites gave selected-area diffraction patterns characteristic of pseudo-boehmite. Prolonged irradiation with the beam produced both an increase in bubble size and density, together with dislocation ejection.

4. Discussion

In the present study it has been shown by the use of combined SE/STE imaging together with conventional SE imaging that the initiation of reaction of aluminium and certain of its alloys with water vapour saturated air at 70° C involves a defilming process which is achieved by surface film blistering. The initial surface film presented to the water vapour must closely resemble the natural oxide, which can be described as a compact barrier layer approximately 10 Å thick covered with a more permeable layer of thickness 50 to 100 Å dependent on storage time at room temperature [11]. The barrier layer has been described as glassy or amorphous [12], but does in fact exhibit an electron diffraction pattern which can be interpreted as poorly ordered γ-Al_2O_3. This, according to Pryor [13] is due to the incorporation of a small number of aluminium ions on anion sites in the pseudo-spinel lattice. Pryor has also suggested that the barrier layer contains an excess of aluminium ions and associated bound electrons to preserve neutrality on cation sites [13]. The starting film however differs from the natural oxide, as the use of electro-polishing as a surface preparative treatment must result in the incorporation of perchlorate ions from the polishing solution [15]. This is unavoidable as the nature of the study involves the preparation of electron-transparent specimens, and alternative methods of preparation would introduce further, more serious, artifacts.

Reaction of the surface film with water vapour saturated air must involve rapid hydration of the film to produce a hydrous oxide (i.e. the precursor of pseudoboehmite) and protons. That this reaction is limited at the barrier layer is suggested by the fact that films with initially thicker porous layers are penetrated and blistered in the same time (i.e. within a few minutes) as freshly prepared films. This ease of hydration of the surface film is not surprising for the reaction is readily reversible as, for example, when pseudoboehmite is heated in air at 300° C it is dehydrated to a poorly crystallized γ-Al_2O_3 [3]. Protons produced at the barrier layer are attracted to the metal–oxide interface which is negatively charged due to the aluminium in excess in the adjacent oxide. At the metal–oxide interface they can be readily discharged and combined to form molecular hydrogen. This process effectively decoheres the interface and surface film blistering is initiated. Blisters are pressurized by the hydrogen gas and extra material for the blister wall is provided by the low density hydrous oxide after the mechanism described by Flower for the reaction of silicon with water vapour [16]. This is shown schematically in Fig. 12a. The compact barrier layer cannot be penetrated by the gas molecules, and hence a high pressure of gas (perhaps of the order of 100 atm. [16, 17]) can develop within the blister.

Growth of the blister proceeds discontinuously,

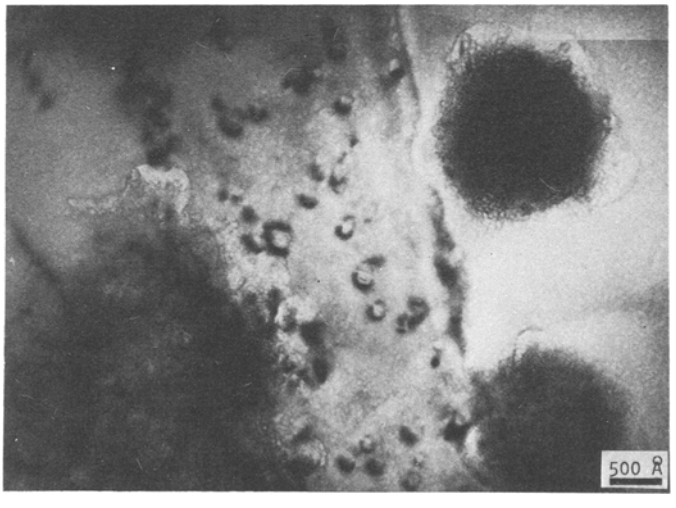

Figure 11 Pseudoboehmite islands at grain boundary–surface intersections on the AlMg alloy after 100 min reaction at 70° C. Bubbles of molecular hydrogen are imaged on the grain boundary by their characteristic strain fields.

as has been similarly reported by Bargeron and Givens [17] from their studies of the reaction of anodically oxidized (800 Å) aluminium surfaces in aqueous chloride media. Their observations, together with the present work and the work of Flower [18] on the electron radiation induced aqueous corrosion of aluminium, suggest blistering of surface films may be a general mechanism of corrosive attack initiation in both aqueous electrolytes and water vapour systems. Discontinuous growth is achieved by continued underpinning of the metal–oxide interface by protons until the bond strength is sufficiently weakened for a burst of blister expansion to occur.

The blister fracture, together with the observed hydroxide growth, is depicted schematically in Figs. 12b and c. Although the final hydroxide film is duplex, it differs from that reported under total immersion conditions at 70° C in that the bayerite somatoids penetrate into the metal rather than being sited above the pseudoboehmite.

The observed effect of magnesium additions both singly (AlMg) and in combination with zinc (AlZnMg) in causing preferential reaction at grain boundary–surface intersections and penetration of hydrogen and of bayerite must be due to its segregation to grain boundaries. Although such grain boundary segregation was not discerned in the present work, recent work by Green *et al.* [19] using electron spectroscopy has directly shown a magnesium-enriched zone, less than 10 Å wide, at grain boundaries in AlZnMg alloys at a level of

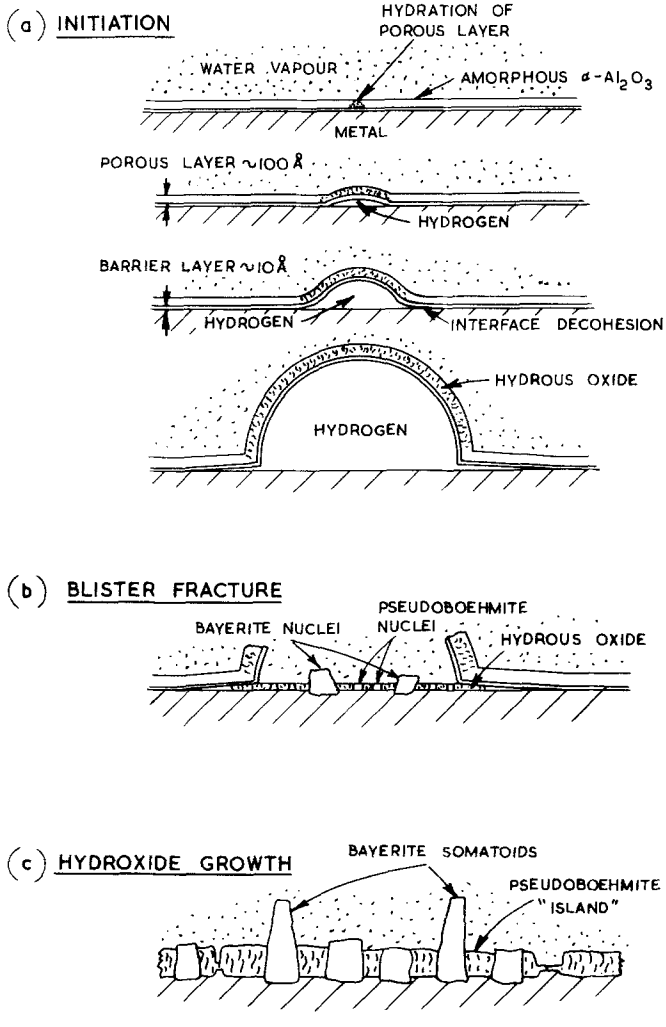

Figure 12 Schematic diagram of reaction occurring at the metal–oxide interface.

segregation that would be beyond the resolution of X-ray microanalysis. This work [19] did not include the effect of solution heat treatment temperature on magnesium segregation. However, Taylor and Edgar [20] have shown, from anodic film studies, that magnesium segregation in AlZnMg alloys decreases as the SHT temperature is raised, and that stress-corrosion cracking susceptibility is correspondingly diminished. Barrier layer anodic oxidation is affected by underlying alloy composition and regions of magnesium segregation produce a thinner final oxide layer. This leads to grain boundary grooves on the surfaces of AlZnMg alloys after solution heat treatment at low temperatures. Magnesium segregation, and hence hydrogen penetration and stress-corrosion susceptibility [21], can therefore be controlled by raising the solution heat treatment temperature. The enrichment of magnesium at grain boundaries must lead to its incorporation in the initial surface film above a boundary site, and this must stimulate hydration and blistering on exposure to WVSA. The fact that not all boundaries are preferential reaction sites even after solution heat treatment at 350° C probably means that magnesium segregation depends on grain boundary type, and may possibly be controlled by alloying additions or treatments which maximize the right type of boundary.

5. Conclusions

The reaction of filmed aluminium surfaces with water vapour saturated air at 70° C is initiated by a hydrogen-induced blistering of the amorphous oxide film. Fracture of the blister results in the development of a circular patch of hydrous oxide. Pseudoboehmite and bayerite nucleate and grow from this "island" of hydrous oxide. The bayerite nucleates at the metal–hydrous oxide interface, and not above the pseudoboehmite as previously reported under conditions of total immersion. Alloying additions of magnesium localize the breakdown reaction to grain boundary surface intersections and this leads to boundary penetration of both hydrogen and bayerite, although this can be prevented by solution heat treatment at 550° C. This may provide a means of control of stress-corrosion susceptibility in AlZnMg alloys.

Acknowledgements

The authors gratefully acknowledge the helpful discussions with Dr W. E. J. Neal, Mr A. T. Thomas, Dr N. C. Davies, Dr C. D. S. Tuck and Dr H. M. Flower held during the course of the work. One of us (A. S. Rehal) was supported by a SRC CASE award.

References

1. G. M. SCAMANS, R. ALANI and P. R. SWANN, *Corros. Sci.* **16** (1976) 443.
2. M. O. SPIEDEL, "The theory of stress corrosion cracking in alloys", edited by J. C. Scully (NATO, Brussels, 1971) p. 289.
3. R. S. ALWITT, "Oxide and oxide films", Vol. 4, edited by J. W. Diggle (Marcel Dekker, New York, 1976) p. 169.
4. R. K. HART, *Trans. Faraday Soc.* **53** (1957) 1020.
5. G. C. BYE and J. G. ROBINSON, *Chem. & Ind.* (1963) 612.
6. W. J. BERNARD and J. J. RANDALL Jr, *J. Electrochem. Soc.* **107** (1960) 483.
7. R. S. ALWITT and L. C. ARCHIBALD, *Corros. Sci.* **13** (1973) 687.
8. W. VEDDER and D. A. VERMILYEA, *Trans. Faraday Soc.* **65** (1969) 561.
9. W. E. NEALE and A. S. REHAL, Symposium on contamination control, Washington, September (1978).
10. G. M. SCAMANS, *J. Mater. Sci.* **13** (1978) 27.
11. M. S. HUNTER and P. FOWLE, *J. Electrochem. Soc.* **103** (1956) 482.
12. F. P. FEHLNER and N. F. MOTT, *J. Oxid. Metals* **2** (1970) 59.
13. M. J. PRYOR, *ibid.* **3** (1971) 271.
14. *Idem, ibid.* **3** (1971) 523.
15. A. F. BECK, M. A. HEINE, E. J. CAULE and M. J. PRYOR, *Corros. Sci.* **7** (1967) 1.
16. H. M. FLOWER and P. R. SWANN, *ibid.* **17** (1977) 305.
17. C. B. BARGERON and R. B. GIVENS, *J. Electrochem. Soc.* **124** (1977) 1845.
18. H. M. FLOWER, *Rad. Effects* **33** (1977) 173.
19. J. M. CHEN, T. S. SUN, R. K. VISWANADHAM and J. A. S. GREEN, *Met. Trans. A* **8A** (1977) 1935.
20. I. T. TAYLOR and R. L. EDGAR, *Met. Trans.* **2** (1970) 833.
21. G. M. SCAMANS and C. D. S. TUCK, Environment-sensitive fracture of engineering materials, TMS–AIME, Chicago (1977).

Received 29 January and accepted 23 March 1979.